

## SYSTEM MODELING FOR A SUPERCRITICAL THERMAL ENERGY STORAGE SYSTEM

Louis Tse<sup>a</sup>, Gani Ganapathi<sup>b</sup>, Richard Wirz<sup>a</sup>, Adrienne Lavine<sup>a</sup>

<sup>a</sup> Mechanical and Aerospace Engineering Dept.  
University of California, Los Angeles  
Los Angeles, CA, USA

<sup>b</sup> Jet Propulsion Laboratory  
California Institute of Technology  
Pasadena, CA, USA

### ABSTRACT

This paper describes a thermodynamic model that simulates the discharge cycle of a single-tank thermal energy storage (TES) system using supercritical fluid in a concentrating solar power plant.

Current state-of-the-art TES design utilizes a two-tank system with molten nitrate salts; one major problem is the high cost of the fluid. The alternate design explored here involves the use of less expensive fluids at supercritical temperatures and pressures. By cycling the storage fluid between a relatively low temperature two-phase state and a high temperature supercritical state, a large excursion in internal energy can be accessed which includes both sensible heat and latent heat of vaporization.

Supercritical storage allows for the consideration of fluids that are significantly cheaper than molten salts; however, a supercritical TES system requires high pressures and temperatures that necessitate a relatively high cost containment vessel that represents a large fraction of the system capital cost. To mitigate this cost, the proposed design utilizes a single-tank TES system, effectively halving the required wall material. A single-tank approach also significantly reduces the complexity of the system in comparison to the two-tank systems, which require expensive pumps and external heat exchangers. However, a single-tank approach also results in a loss of turbine power output as the storage fluid

temperature declines over time during the discharge cycle.

The thermodynamic model is used to evaluate system performance; in particular it predicts the reduction in energy output of the single-tank system relative to a conventional two-tank storage system. Tank wall material volume is also presented and it is shown that there is an optimum average fluid density that generates a given turbine energy output while minimizing the required tank wall material and associated capital cost.

Overall, this study illustrates opportunities to further improve current solar thermal technologies. The single-tank supercritical fluid system shows great promise for decreasing the cost of thermal energy storage, and ensuring that renewable energy can become a significant part of the national and global energy portfolio.

### NOMENCLATURE

$c_p$	specific heat of HTF ( $\text{J kg}^{-1}\text{K}^{-1}$ )
$E$	energy (J)
$m$	storage fluid mass (kg)
$\dot{m}$	mass flow rate ( $\text{kg s}^{-1}$ )
$P$	pressure (kPa)
$q$	heat rate (W)

$T$	temperature ( $^{\circ}\text{C}$ )
$u$	internal energy per unit mass ( $\text{J kg}^{-1}$ )
$\varepsilon$	internal heat exchanger effectiveness
$\eta$	power plant efficiency
$\rho$	fluid average density ( $\text{kg m}^{-3}$ )
CSP	concentrating solar power
HTF	heat transfer fluid
TES	thermal energy storage

## SUBSCRIPTS

$b$	bypass
$c$	critical
$gen$	generator
$in$	inlet
$out$	outlet
$stor$	storage
$tank$	tank (refers to HTF flowing through tank)
$turb$	turbine

## INTRODUCTION

Solar thermal technology is viewed as the most cost-effective option to convert solar radiation into electricity and it has been operationally proven since the mid-1980s. The thermal energy storage (TES) subsystem is an integral element in concentrating solar power (CSP) plants that mitigates short-term intermittency in solar insolation. The Department of Energy has identified improved thermal energy storage as one of the critical technology developments needed to allow solar thermal power to replace non-renewable power generation sources [1]. This paper addresses a proposed supercritical fluid thermal energy storage system. In particular, it explores the behavior and optimization of such a system during the discharge cycle, when the storage fluid provides thermal energy to the steam generator.

The current state-of-the-art TES design utilizes a two-tank indirect storage system with molten nitrate salts. However, the salt mixtures used for these systems, which are typically a mixture of sodium nitrate (60 wt%) and potassium nitrate (40 wt%), can be prohibitively expensive. Results of studies from Kolb [2], Van Lew [3], and Pacheco [4] show that alternative designs, such as thermocline indirect storage systems, are being

developed and are economically competitive when compared to two-tank molten salt systems.

The alternative design explored here [5] involves a supercritical TES system that utilizes fluids that are significantly less expensive than molten salts. By cycling the storage fluid between a relatively low temperature two-phase state and a high temperature supercritical state, a large excursion in internal energy can be accessed which includes both sensible heat and latent heat of vaporization.

The main challenge to such a system is the large pressure associated with the high temperature state, necessitating a thick-walled containment for the storage fluid. The wall material cost is a major capital cost of the TES system. To mitigate this cost, the proposed design utilizes a single-tank TES system, effectively halving the required wall material. A preliminary cost estimate suggests that this design may noticeably reduce costs when compared to the state-of-the-art two-tank molten salt design [5].

In the proposed single-tank design (see schematic, Figure 1), the storage fluid is enclosed in tube bundles with sufficient wall thickness to withstand the highest system pressure. The tube bundles are contained in a low-pressure tank shell, through which the heat transfer fluid (HTF) flows, creating a heat exchanger internal to the storage tank. Another study is exploring the complicated heat transfer mechanisms that are occurring within a single tube during the charging and discharging cycle, such as cell convection, phase change, and dynamic heat transfer properties near the critical point [6]. Additionally, a small-scale demonstration of the single-tank design will be constructed by the Jet Propulsion Laboratory [7].

The schematic shows the operation during the discharge cycle, when the HTF flows between storage and the steam generator. During charging, the HTF is directed to flow between storage and the solar field.

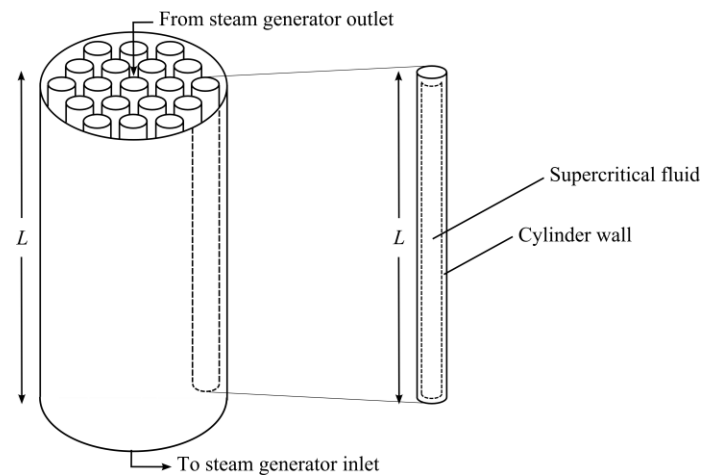


**Figure 1:** Single-tank system configuration with tube bundles.

The primary advantage to the supercritical design, as mentioned previously, is the reduction in fluid costs. Additionally, the integration of system components into a single tank with internal heat exchanger removes the need to pump the storage fluid between two tanks through an external heat exchanger, eliminating the capital cost of an external heat exchanger rated for supercritical pressures, a supercritical pump, the associated pumping costs, and related heat losses from the system.

The use of a single-tank design does, however, result in one disadvantage relating to power production during the discharge cycle. In a two-tank system, the storage fluid and HTF pass through an external heat exchanger, and the cooled storage fluid is segregated in a separate tank. The storage fluid remaining in the high temperature tank retains a constant temperature, so that the steam generator can always operate at its design conditions. In contrast, in the single-tank design the storage fluid remains in a single tank through which the HTF flows; as a result the storage fluid temperature declines with time. Large-scale turbines are commercially available that allow for the use of steam within a temperature range (as opposed to a fixed design rating), but at the cost of lower efficiency as the steam temperature declines. This loss of efficiency can be avoided if the high temperature state of the storage fluid is hot enough, but this also means the pressure will have to be higher, leading to increased tank material costs.

The objective of this paper is to simulate the discharge cycle using the single-tank system, and to calculate the turbine power output when it is drawing from storage. The nominal design generates 50 MWe for a 12-hour period. It will be shown that there is an optimum average fluid density that generates a given energy production while minimizing the required tank wall material and associated capital cost.

## SYSTEM MODEL

The thermal energy storage unit interacts with the charging and discharging loops, as shown in Figure 2. In the charging loop, energy from the solar field is transferred to the tube bundles containing the storage fluid via heat transfer from the HTF. The discharging loop reverses this process and removes energy from the tube bundles to the HTF, to produce steam for power generation. This paper addresses the discharge portion of the cycle only. Other studies investigate a range of different aspects, such as the charging cycle (Powell & Edgar, 2012 [8]), storage tank design (Gabielli & Zamparelli, 2009 [9]), parabolic trough performance (Forristall, 2003 [10]), power cycle efficiency (McMahan et al 2007 [11]), and system operation (Esen & Teoman, 1996 [12]).

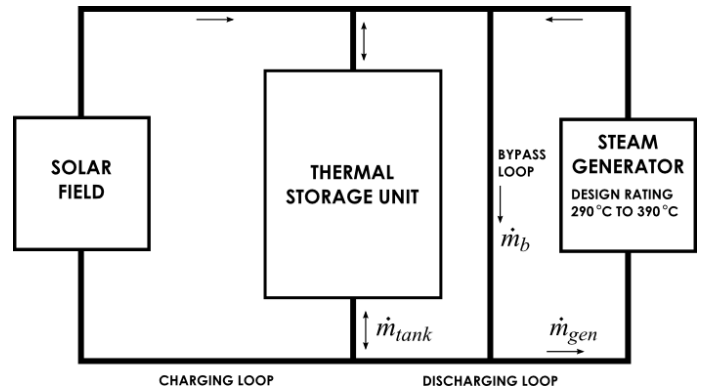


**Figure 2:** Basic thermal energy storage system components.

Since the storage fluid temperature is very high at the beginning of the discharge cycle, the HTF temperature will also be higher than the optimal value required by the steam generator; this value is taken as 390°C based on a performance study of a two-tank TES system performed by Kolb [2]. To reduce the HTF temperature to its design value, the HTF exiting the thermal storage unit is mixed with the HTF exiting the steam generator through a bypass loop.

The thermal storage tubes are loaded with a certain fixed mass of the storage fluid. Since their volume remains constant, the average density  $\rho$  also remains constant. Thus the discharge cycle follows a constant density (i.e. constant specific volume) line on a  $P$ - $v$  diagram, as shown in Figure 3. The discharge process begins at a supercritical state corresponding to high temperature, pressure, and internal energy, and ends at a two-phase state at lower temperature, pressure, and internal energy. At any instant in time, the internal energy and density can be related to the storage fluid temperature and pressure:

$$u = u(T_{stor}, P), \quad \rho = \rho(T_{stor}, P) \quad (1, 2)$$

Thus with fixed density, if the storage fluid temperature is known, its pressure can be determined from Eq. (2) and its internal energy can then be determined from Eq. (1). These relationships are implemented using the Peng-Robinson equation of state, which has been shown to provide reasonable predictive capabilities for a wide range of fluids [13]. Additional needed inputs for Eqs. (1) and (2) are the fluid critical temperature and pressure, acentric factor, and the ideal gas specific heat and saturation pressure as functions of temperature. In this paper, naphthalene is used as the storage fluid. The ideal gas specific heat is generated as a curve fit to the data of Barrow and McClellan [14], and the saturation pressure is modeled using the Pitzer correlation [15].

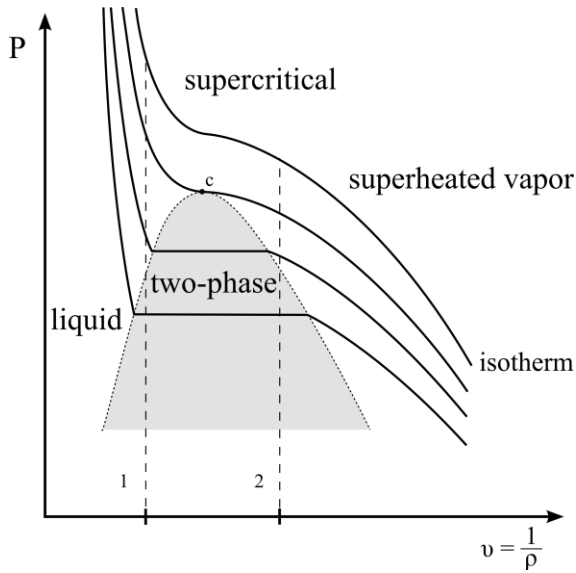


**Figure 3:**  $P$ - $v$  diagram showing vertical lines of constant average fluid density.

The thermal storage unit and discharge loop are modeled with a set of energy and mass balances, as given below.

Transient energy balance on the storage fluid:

$$m \frac{du}{dt} = q_{stor} \quad (3)$$

where  $q_{stor}$  is negative, corresponding to energy leaving the storage fluid.

Energy balance between the storage fluid and the HTF:

$$q_{stor} = \dot{m}_{tank} c_p \varepsilon (T_{tank,in} - T_{stor}) \quad (4)$$

Equation (4) assumes that the storage fluid temperature is spatially uniform and therefore the heat exchanger can be treated as if it were a single-stream heat exchanger, characterized by an effectiveness,  $\varepsilon$ .

Energy balance for the HTF flowing through the storage tank:

$$q_{stor} = \dot{m}_{tank} c_p (T_{tank,in} - T_{tank,out}) \quad (5)$$

Energy balance for the HTF flowing within the discharge loop (assuming no losses in the piping):

$$\dot{m}_{gen} T_{gen,in} = \dot{m}_b T_{gen,out} + \dot{m}_{tank} T_{tank,out} \quad (6)$$

Equality of the HTF temperature at the generator outlet and the tank inlet (assuming no losses in the piping):

$$T_{tank,in} = T_{gen,out} \quad (7)$$

Energy balance for the HTF flowing through the steam generator:

$$q_{gen} = \dot{m}_{gen} c_p (T_{gen,in} - T_{gen,out}) \quad (8)$$

Mass balance for the HTF:

$$\dot{m}_{gen} = \dot{m}_b + \dot{m}_{tank} \quad (9)$$

In addition, the operation of the bypass loop must be modeled. The steam generator is designed to operate with  $T_{gen,in} = 390^\circ\text{C}$ . As long as the HTF temperature exiting the storage tank ( $T_{tank,out}$ ) remains higher than this value, the bypass loop is used to mix the hotter inlet fluid with colder fluid from the steam generator outlet (see Figure 2); the required value of  $\dot{m}_b$  is calculated from Eq. (6) with  $T_{gen,in} = 390^\circ\text{C}$ . When  $T_{tank,out}$  reaches  $390^\circ\text{C}$ , the bypass loop is not used. The bypass mass flow rate is set to zero and Eq. (6) is solved for  $T_{gen,in}$ , which drops below the design value. Thus, the bypass operation is modeled as a function of time during the discharge by augmenting Eqs. (1-9) with the following:

$$T_{gen,in} = 390^\circ\text{C} \text{ and solve for } \dot{m}_b \text{ (for } \dot{m}_b > 0) \quad (10a)$$

$$\dot{m}_b = 0 \text{ and solve for } T_{gen,in} \text{ (thereafter)} \quad (10b)$$

Finally, the behavior of the steam generator must be modeled, taking into account how its performance varies as the HTF temperature at the generator inlet declines below its design value. Kolb [2] conducted a study evaluating the system performance of two-tank and thermocline thermal storage systems. This study developed an empirical model of an operating Andasol-type power generation facility utilizing a “sliding” temperature turbine, and provided graphs of steam generator outlet temperature and turbine power output as functions of steam generator inlet temperature and mass flow rate. Here, curve fits to his data are used for the maximum (design value) of HTF flow rate through the generator, namely  $\dot{m}_{gen} = 547 \text{ kg/s}$ . The results are:

$$T_{gen,out} = 0.433(T_{gen,in} - 390^\circ\text{C}) + 289^\circ\text{C} \quad (11)$$

$$q_{turb} = 0.344T_{gen,in} - 84.16 \quad (12)$$

Note that Eqs. (11) and (12) are only valid provided that the steam generator is operating within an allowed range, namely  $300^\circ\text{C} < T_{gen,in} < 390^\circ\text{C}$ ; all cases simulated were maintained within this range. These equations correspond

to a turbine that generates 50 MWe under design conditions at 37% efficiency, with  $T_{gen,in} = 390^\circ\text{C}$ . Note that the efficiency of the power system is  $\eta = q_{turb} / q_{gen}$ , which is a decreasing function of  $T_{gen,in}$  due to the steam generator receiving fluid at temperatures lower than its design condition.

Once the discharge model is solved for a specified period of time, the quantity of thermal energy removed from storage,  $E_{stor}$ , can be calculated:

$$E_{stor} = m\Delta u \quad (13)$$

where  $\Delta u$  is the difference in specific internal energy between the initial and final states. The importance of this equation is that  $E_{stor}$  also represents the quantity of solar energy that had to be diverted to storage during the charge portion of the cycle. Under design conditions, the value of  $E_{stor}$  needed to generate the desired turbine power of 50 MWe for 12 hours at the maximum efficiency of 37% is  $E_{stor} = 50 \text{ MW} \times 12 \text{ h} / 0.37 = 1621 \text{ MWh}$ .

Within Eqs. (1)-(13), parameters that describe the storage fluid, the HTF, and the internal heat exchanger effectiveness are fixed as shown in Table 1. In addition, the discharge time period is fixed at 12 hours, and the stored energy,  $E_{stor}$ , is fixed at the corresponding value of 1621 MWh. Two parameters will be varied: the fluid loading, or average density  $\rho$ , and the initial storage fluid temperature.

**Table 1:** System specifications of the TES system.

Fixed parameters	
Storage fluid	Naphthalene ( $P_c = 4070 \text{ kPa}$ , $T_c = 478^\circ\text{C}$ )
Heat transfer fluid specific heat, $c_p$	2.5 kJ/kg
Heat transfer fluid mass flow rate, $\dot{m}_{gen}$	547 kg/s
Internal heat exchanger effectiveness, $\varepsilon$	0.9
Discharge time period	12 hours
Storage capacity	1621 MWh
Varied parameters	
Storage fluid loading, $\rho$	Baseline value: 400 kg/m <sup>3</sup> Range: 200 to 600 kg/m <sup>3</sup>
Initial storage temperature	Baseline value: 500°C Range: 420 to 500°C

The system model was implemented in the simulation program Engineering Equation Solver (EES) because it enables solution of simultaneous equations, including differential equations, and contains the Peng-Robinson

equation of state as a built-in function. The time step size for the calculations was 10 s, which was chosen after careful examination that smaller time steps did not show noticeable change in the results.

## NUMERICAL RESULTS AND DISCUSSION

The simulation results for the baseline system are presented in Figure 3, which illustrates the transient behavior of the system during the discharge cycle.

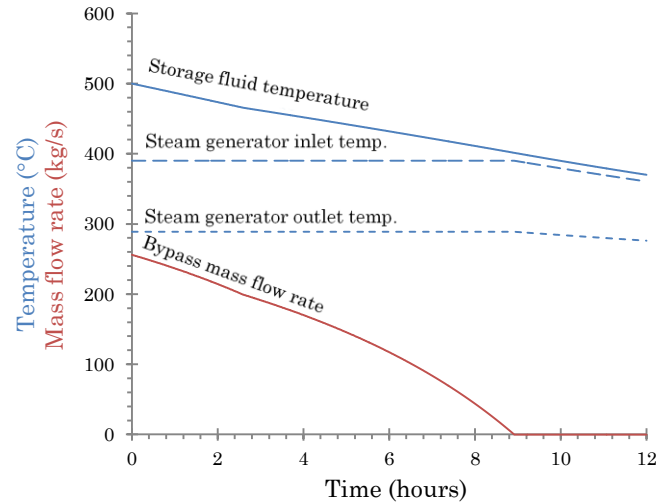


**Figure 3:** Temperature and bypass flow rate behavior during the discharge cycle.

It can be seen that the HTF temperature at the generator inlet,  $T_{gen,in}$ , remains higher than  $390^\circ\text{C}$  for approximately nine hours and is mixed with the appropriate volume of colder HTF through the bypass loop from the steam generator outlet. This results in the steam generator receiving fluid at its design rating of  $390^\circ\text{C}$  for maximum efficiency. In this region, the TES system generates 429 MWh (see Figure 4), which is equivalent to the energy output that a two-tank system can generate in the same amount of time. After this point,  $T_{gen,in}$  becomes gradually less than  $390^\circ\text{C}$  and is no longer mixed with colder HTF from the steam generator outlet (the bypass loop is closed). Naturally the power output declines during this period following Eqs. (11) and (12). During this latter part of the discharge cycle, the system produces 150 MWh. In total, the single tank TES system produces approximately 580 MWh. When compared to a two-tank system (which produces the design value of 600 MWh over a 12 hour period), the energy loss is only about 3.3%.

Next, a series of numerical simulations was conducted to assess the impact of storage fluid loading (or average density,  $\rho$ ). Varying  $\rho$  corresponds to traversing

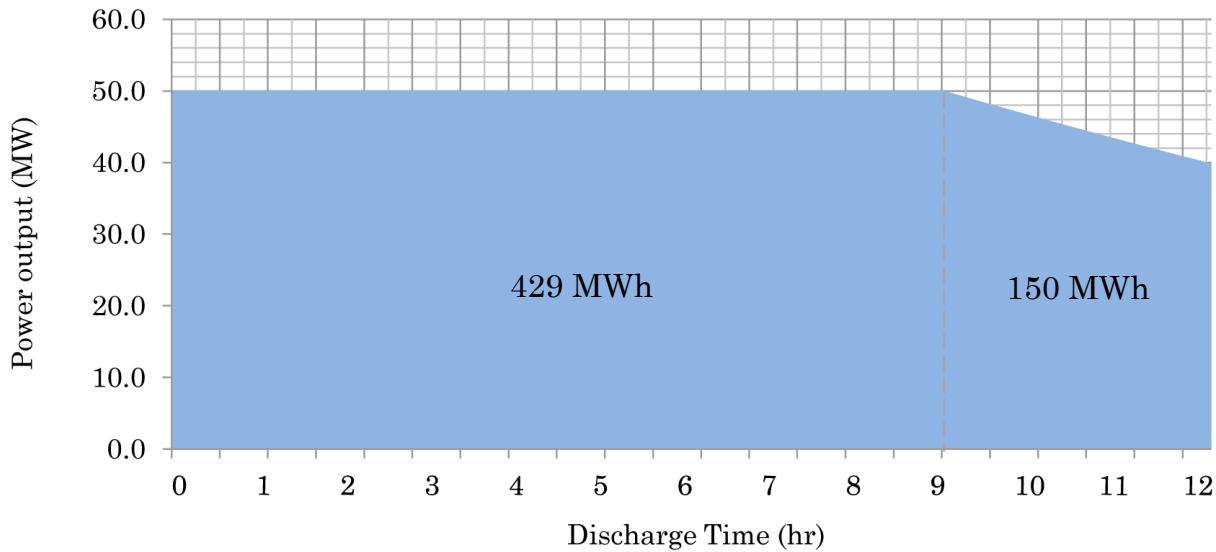


**Figure 4:** Power and energy output of the single tank system during the discharge cycle.

the  $P$ - $v$  diagram (Figure 3) along different vertical lines. Higher fluid density is beneficial because it corresponds to larger energy storage density, i.e. the required thermal energy can be stored in a smaller volume. However, increasing fluid density also has the negative impact of increasing maximum system pressure (holding maximum temperature fixed); for example, in Figure 3, the initial (maximum) pressure for path 1 (high density) is higher than the initial pressure for path 2 (low density) starting at the same initial temperature.

The results of the simulation are shown in Table 2. It should be noted that the energy output reduction for all these cases is the same as for the baseline ( $\rho = 400 \text{ kg/m}^3$ ), namely 3.3%. The results confirm that the required storage fluid volume lessens with higher fluid density. This means that the tubes may be smaller (or fewer can be used). However, pressure increases rapidly as fluid density increases; this means that the tubes must have higher wall thicknesses to withstand the higher pressures. Clearly, when considering the capital cost associated with the tube wall material, there is a trade-off between having lesser storage fluid volume, but greater wall thickness.

**Table 2:** Discharge cycle results for varying fluid density (for fixed energy storage capacity of 1621 MWh and initial temperature of 500°C).

Fluid density ( $\text{kg/m}^3$ )	Maximum pressure (kPa)	Fluid volume ( $\text{m}^3$ )	Fluid mass (kg)	Tube wall material volume ( $\text{m}^3$ )
200	4531	73,500	$14.7 \times 10^6$	9440
300	5036	51,667	$15.5 \times 10^6$	7400
400	6014	41,500	$16.6 \times 10^6$	7144
500	8945	35,800	$17.9 \times 10^6$	9344
600	16,292	32,667	$19.6 \times 10^6$	16,269

To quantify this effect, the tube wall material volume was calculated and is shown in the last column. The tube material volume is calculated from the storage fluid volume, as well as the wall thickness required to withstand the maximum pressure. The required wall thickness can be determined using the expression for hoop stress in a thin-walled cylinder. The result is expressed as:

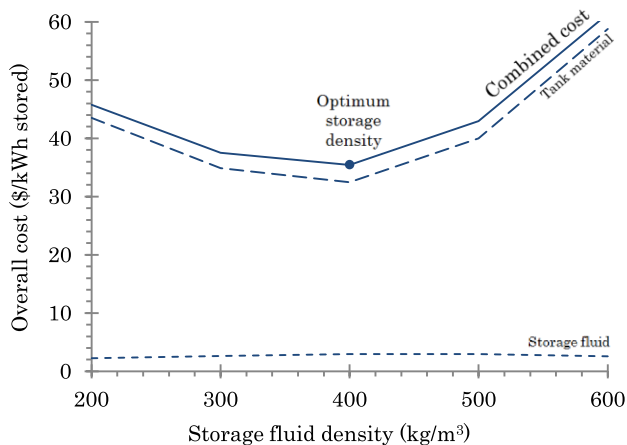
$$t_w = \frac{nPr}{F_{tu}} \quad (14)$$

where  $n$  is the safety factor,  $P$  is the maximum pressure,  $r$  is the inner radius, and  $F_{tu}$  is the allowable tensile strength with a derating factor due to high temperature loading. A safety factor of 3 is used, and the tensile strength is for SS316L per Military Standardization Handbook 5 data [16]. It can be seen in Table 2 that there is an optimum fluid density, at approximately  $400 \text{ kg/m}^3$ , at which point the total tube bundle wall material volume (and thus, capital cost) is at a minimum.

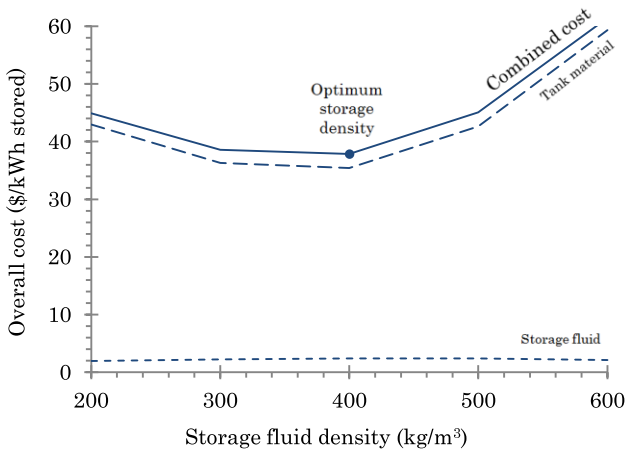
It can also be noted that the storage fluid mass corresponds to the capital cost of filling the tube bundles with the storage fluid. However, for the inexpensive fluids anticipated in this study, the fluid cost is negligible compared to the tank wall material. For example, for naphthalene in a tank made of SS316L, the fluid cost would be on the order of 15% of the tank wall material cost. Additionally, the required storage fluid volumes in Table 2 are comparable to two-tank TES systems of the same capacity. An engineering study of molten salt storage, evaluated by Hermann et al. [17] and tested in the Solar Two project, shows that the combined volume of the cold and hot tank is approximately  $60,000 \text{ m}^3$  for a system with similar energy storage capacity. This

illustrates that the single-tank design requires less storage fluid volume.

Further simulations were conducted to observe the behavior of the optimum storage fluid density as system parameters change. The effect of lower initial temperature is shown in Figure 5.



(a)



(b)

**Figure 5:** Optimum storage density remains at approximately  $400 \text{ kg/m}^3$  for maximum storage temperature of a)  $480^\circ\text{C}$  and b)  $500^\circ\text{C}$ .

It can be seen that the optimum storage fluid density remains at approximately  $400 \text{ kg/m}^3$ , for which the capital cost of the tube bundle material reaches a minimum. Moreover, the energy output reduction remains the same, at 3.3%. Due to the lower initial temperature, greater storage fluid mass is needed to maintain the same energy storage capacity, but as mentioned before, the cost of the fluid is much less than the tube wall material cost. Interestingly, the tube wall material volume is less for the case with a starting temperature of  $480^\circ\text{C}$ ; this illustrates that there are complex interactions between system parameters that require cost optimization.

The goal of the next parametric study was to observe the influence of initial storage temperature, and determine the optimum value to minimize tank cost. Using the

result from the previous simulations, the optimum storage fluid density and energy storage capacity is kept constant while varying initial storage temperature. The effect of initial storage temperature is shown in Figure 6.

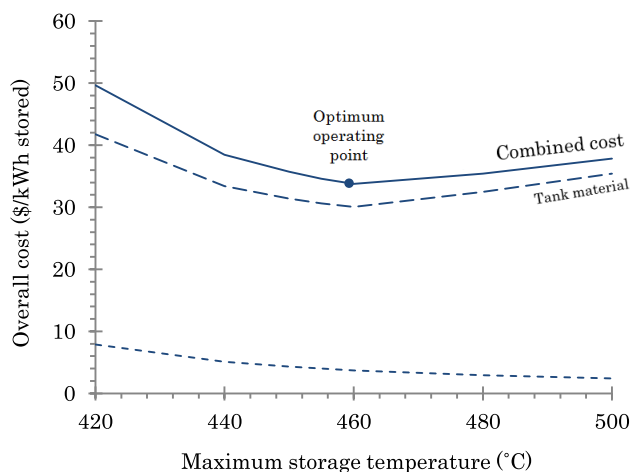


**Figure 6:** Maintaining storage fluid density at  $400 \text{ kg/m}^3$ , the optimum maximum storage temperature is approximately  $460^\circ\text{C}$ .

Maintaining storage fluid density at the optimum value of  $400 \text{ kg/m}^3$ , the optimum maximum storage temperature for minimizing cost is approximately  $460^\circ\text{C}$ . Overall, the influence of storage fluid density is much greater than that of maximum storage temperature, which will inform decision-making in the design process.

## CONCLUSION

This paper presents a thermodynamic model that evaluates the system performance of a single-tank TES system utilizing supercritical fluids in a CSP plant. This system model has been used to determine the effects of fluid density on system pressure, required storage volume, and tube material volume for a fixed energy storage capacity. Based on these simulations, the results show that an optimum fluid density can be determined for minimizing tube material volume, and consequently, capital costs. The model can be particularly useful in 1) system design, and 2) optimization of discharge cycle strategies. This study indicates the presence of opportunities to further optimize current solar thermal energy storage designs.

For further work, the system model can be utilized to perform optimization analysis on various system specifications to attain a balance between system performance and overall cost. Future simulations will investigate additional variables and conduct parametric studies to observe the behavior of the system in more detail. The methodology of analyzing the thermoeconomic performance of the single-tank TES system will tie each parameter according to their

respective costs to illuminate the system components that contain greater opportunity for optimization. Additionally, the system can be modeled using various fluids in combination with market analysis to determine the most cost-effective storage fluid candidate. In addition, TES systems operating with low or mid-temperature ranges (200°C – 300°C) can be modeled to study power plants operating in those temperature ranges. The charging cycle will also be a topic for future investigation.

## ACKNOWLEDGEMENTS

This effort was supported by ARPA-E Award DE-AR0000140 and Grant No. 5660021607 from the Southern California Gas Company.

## REFERENCES

1. Advanced Research Projects Agency – Energy. “High Energy Advanced Thermal Storage (HEATS). [Online]. Available: <http://arpa-e.energy.gov/ProgramsProjects/HEATS.aspx>. [Accessed: 10-Jan-2012].
2. Kolb, Gregory J. “Evaluation of annual performance of 2-tank and thermocline thermal storage systems for trough plants,” *Journal of Solar Energy Engineering*, Vol. 133, August 2011.
3. Van Lew, Jon T., Li, Peiwen, Karaki, Wafaa, Stephens, Jake. “Analysis of Heat Storage and Delivery of a Thermocline Tank Having Solid Filler Material,” *Journal of Solar Energy Engineering*, Vol. 133, 2, 2011.
4. Pacheco, James E., Showalter, Steven K., Kolb, William J. “Development of a Molten-Salt Thermocline Thermal Storage System for Parabolic Trough Plants,” *Journal of Solar Energy Engineering*, Vol. 124, 2, pp. 153-159, 2002.
5. Ganapathi, G.B., Wirz, R.E. “High density Thermal Energy Storage with Supercritical Fluids”, ASME 2012 6th International Conference on Energy Sustainability, Jul 23-26, San Diego, CA, USA (submitted).
6. Choi, D., Wirz, R. E., Ganapathi, G. B., Kavehpour, H. P. “Analysis and Considerations for Thermal Storage Using Novel Supercritical Fluids,” ASME 6th International Conference on Energy Sustainability, July 23-26, 2012, San Diego, California, USA.
7. Ganapathi, G. B., Berisford, D., Pauken, M., Wirz R.E. “A 5 kWh Lab Scale Demonstration of a Novel Thermal Energy Storage Concept with Supercritical Fluids,” ASME 6th International Conference on Energy Sustainability, July 23-26, 2012, San Diego, California, USA.
8. Powell, Kody M., Edgar, Thomas F. “Modeling and control of a solar thermal power plant with thermal energy storage.” Elsevier, *Chemical Engineering Science*, Vol. 71, pp. 138-145, March 2012.
9. Gabrielli, R., Zamparelli. “Optimal Design of a Molten Salt Thermal Storage Tank for Parabolic Trough Solar Power Plants,” *Journal of Solar Energy Engineering*, Vol. 131, 4, 041001, 2009.
10. Forristall, R. “Heat transfer analysis and modeling of a parabolic trough solar receiver implemented in Engineering Equation Solver.” National Renewable Energy Laboratory Technical Report NREL/TP-550-34169, 2003.
11. McMahan, A., Klein, S.A., Reindl, D.T. “A finite-time thermodynamic framework for optimizing solar-thermal power plants.” *Journal of Solar Energy Engineering*, Vol. 129, 4, pp. 355-363, 2007.
12. Esen, Mehmet, Ayhan, Teoman. “Development of a model compatible with solar assisted cylindrical energy storage tank and variation of stored energy with time for different phase change materials.” *Energy Convers. Mgmt*, Vol. 37, 12, pp. 1775-1785, 1996.
13. Peng, Ding-Yu, Robinson, Donald B., “A new two-constant equation of state.” *Ind. Eng. Chem. Fundamen.*, Vol. 15, 1, pp. 59-64, 1976.
14. Barrow, G.M., McClellan, A.L. “The thermodynamic properties of naphthalene.” *J. Am. Chem. Soc.*, Vol. 73, pp. 573-575, 1951.
15. Pitzer, K.S. “Ion interaction approach: Theory and data correlation.” *Activity coefficients in electrolyte solutions*, CRC Press, 1991.
16. Military Standardization Handbook, MIL-HDBK-5B. “Metallic Materials and Elements for Aerospace Vehicle Structures.” September 1971.
17. Herrmann, Ulf, Kelly, Bruce, Price, Henry. “Two-tank molten salt storage for parabolic trough solar power plants,” Elsevier, *Energy*, Vol. 29, 5-6, pp. 883-893, 2004.